

Potential energy surface of In and Ga adatoms above the (111)A and (110) surfaces of a GaAs nanopillar

J. N. Shapiro, A. Lin, and D. L. Huffaker

California Nanoscience Institute and Electrical Engineering Department, University of California at Los Angeles, Los Angeles, CA 90095, USA

C. Ratsch

Institute for Pure and Applied Mathematics and Department of Mathematics, University of California at Los Angeles, Los Angeles, CA 90095, USA

(Received 9 February 2011; revised manuscript received 3 August 2011; published 29 August 2011)

Density-functional calculations of the potential-energy surface for tracer Ga and In adatoms above two GaAs (111)A and two GaAs (110) surface reconstructions are presented in order to understand the growth conditions required to form axial GaAs/InGaAs heterostructures in nanopillars. The surface reconstructions present under As-rich conditions have lower diffusion barriers for In adatoms. In addition, the binding energy of In becomes more competitive with Ga under As-rich conditions. We conclude that the As-rich reconstructions for GaAs(110) and GaAs(111)A are preferable for selective formation of heterointerfaces on (111) facets. This work helps explain the recent successful formation of axial GaAs/InGaAs heterointerfaces in catalyst free nanopillars.

DOI: [10.1103/PhysRevB.84.085322](https://doi.org/10.1103/PhysRevB.84.085322)

PACS number(s): 68.43.Jk, 68.35.Fx

I. INTRODUCTION

Semiconductor nanowires (NWs) and nanopillars (NPs) are exciting materials for probing mesoscopic physics and as building blocks for future high-performance optoelectronic devices on Si.¹⁻³ NP synthesis by catalyst-free selective-area metal-organic chemical vapor deposition (SA-MOCVD) is a growth technique for forming large arrays of uniform NPs in lithographically defined locations. The precision with which the NPs can be positioned can be utilized for fabrication of photonic crystals or electronic devices requiring precision lithography and alignment.⁴⁻⁶

The absence of a metal particle to catalyze growth means that atoms adsorb directly onto the crystal surfaces from the vapor, and the resulting crystal shape is controlled in part by minimization of the total surface free energy.⁷ GaAs nanopillars grow in the [111] direction, and have hexagonal symmetry with side facets composed of the six (01 $\bar{1}$) planes. Atoms from the vapor adsorb on all facets of the NP and then diffuse to the (111) surface at the tip where they incorporate. The polar (111) surface has a higher surface energy than the stoichiometric {011} family, making the observed crystal shape thermodynamically favorable. However, the vertical growth of nanopillars has a strong temperature dependence, so adatom kinetics and surface reaction rates must also play an important role in epitaxy.

Heterostructure formation is a necessary capability to master in catalyst-free NP synthesis in order to create efficient optical devices.⁸ Core-shell heterostructures have been studied in a variety of material systems, but axial heterostructure formation has been elusive in this growth mode. When a new atomic species is introduced, the surface energetics must promote incorporation of the new species on the top (111) surface while simultaneously suppressing nucleation on the side walls.

Despite this challenge, axial InGaAs segments of varying composition and thickness were recently demonstrated in GaAs catalyst free NPs grown by SA-MOCVD.⁹ High As

flow rates were required to promote incorporation of In on the NP tip with negligible shell growth. At the lower As flow rates typically used for GaAs NP homoepitaxy, In is not selective to the (111) surface, and instead nucleates on the sidewalls, deforming the crystal facets. Fig. 1(a) shows scanning electron micrograph (SEM) of NPs formed by SA-MOCVD with axial InGaAs inserts formed at high As flow rates. The vertical side walls and hexagonal symmetry are evident. Figure 1(b) shows a dark-field scanning transmission electron micrograph (STEM) of the same pillars revealing the axial InGaAs segment. In contrast, Fig. 1(c) shows pillars terminated with InGaAs at low As flow rates. These pillars have deformed crystal facets due to In nucleation on the side walls. This tendency for In to bond to all available crystal surfaces has also been reported in Ref. 10.

To investigate possible reasons for the observed difference in behavior between In and Ga during nanopillar epitaxy, we present a theoretical investigation of the potential energy surface (PES) for Ga and In tracer adatoms situated above the stable (111)A and (110) surfaces of an NP. The stable surfaces at both high and low As chemical potential are investigated to parallel the experimental conditions of high and low As flow rates. The technique of calculating a PES has been applied by numerous researchers as a tool for studying diffusion, adsorption and desorption and for understanding epitaxy on crystal surfaces.¹¹⁻¹⁷

In this study, the diffusion barriers and binding energies of In and Ga adatoms are computed and compared to determine the mobility of each species on the surface, and to glean insight into the physical processes that determine the preferred facet for heteroepitaxy. The surfaces under consideration are pure GaAs, therefore the calculations are relevant to nucleation of the first layer of InGaAs on a free-standing GaAs NP.

The computational methods are discussed first, followed by a description of the calculations and their results. We conclude with a discussion and interpretation of the results.

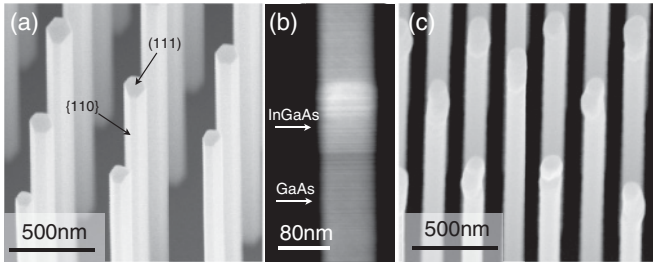


FIG. 1. (a) SEM of GaAs nanopillars containing axial InGaAs inserts grown at high V/III ratio. (b) Dark-field STEM of single InGaAs insert. (c) SEM of GaAs nanopillars terminated with InGaAs at low V/III ratio.

II. COMPUTATIONAL METHODS

A potential energy surface (PES) calculation for a Ga or In adatom begins with the computation of the equilibrium surface geometry without the adatom. The surfaces under consideration are the (111)A and (110) surfaces. The top and side views of each surface are shown in Fig. 2. The NP side walls are actually the six $(\bar{1}10)$ surfaces, but these are structurally identical to the (110) surface under investigation. The (111)A Ga vacancy and (110) Ga-As chain are stable under As-poor conditions when the As chemical potential is low. The (111)A As trimer and (110) As-As chain are stable

under As-rich conditions when the As chemical potential is high.^{18,19}

The (111) surfaces have a 2×2 unit cell indicated by a shaded parallelogram, and the (110) surfaces have a 1×1 unit cell indicated by a shaded rectangle. In our calculations, the (111) slabs are nine monolayers thick and the (110) slabs are eight monolayers thick. All surfaces are iteratively relaxed, keeping the bottom three monolayers fixed, until residual atomic forces are <0.02 eV \AA . After the relaxed surface is computed, the PES can be computed by finding the total energy of the surface with a single adatom at different points above the surface.

The total energy of the surface with an additional Ga or In adatom is computed using a larger super cell to suppress interaction between the adsorbates. The top layers of the slab and the adatom are allowed to relax, but the adatom coordinates are fixed perpendicular to the [111] direction (the adatom is fixed in the xy plane and allowed to relax in z). The two (111) surfaces have threefold rotational symmetry, and each rotationally symmetric slice has a mirror symmetry such that only eight points are sampled in a triangle above the 2×2 unit cell. The calculated energies are reflected, rotated twice through 120° , and mapped to a rectilinear grid using a cubic interpolation to generate a PES for the adatom of interest. The energy zero point is chosen to be the total energy of the relaxed, reconstructed surface plus the total energy of an isolated atom of In or Ga.

A similar process is used to calculate the PES for the (110) surfaces, but these surfaces are simpler because they only have a mirror symmetry. The lowest energy site for these surfaces, however, does not lie in a region of high symmetry. To find the true potential minimum, the adatom is placed at the site with the lowest energy and allowed to relax without positional constraints.

Calculations are performed within the framework of density-functional theory (DFT) as implemented in the software package FHI-AIMS,²⁰ which uses numeric atom centered orbitals for its basis set and includes a relativistic correction for heavy atoms ($Z > 30$). The Perdew-Burke-Ernzerhof (PBE) parametrization of the generalized gradient approximation is used for the exchange-correlation functional.²¹ Approximately 16 layers of vacuum and 64 equivalent k points in the 1×1 unit cell are specified. Convergence of the energy difference between the maximum and minimum on the PES is confirmed for the k points, slab thickness, vacuum layers, and supercell size for the Ga vacancy and the Ga-As chain surface.

Calculations were performed using the FHI-AIMS predefined “light” setting. In the “light” setting, each atom has radial basis functions of s , p , and d character with an overall cutoff radius of 5 \AA and a local Hartree potential expansion up to $l = 4$. Key results were tested for convergence by calculation with the predefined “tight” setting. In the “tight” setting, each atom has a finer integration grid, an additional f -like basis function, an overall cutoff radius of 6 \AA , and a local Hartree potential expansion up to $l = 6$. The binding energy difference for a Ga adatom at the maximum and minimum of the Ga vacancy PES is 1.056 eV using “light” and 1.051 eV using “tight” settings. Calculations are therefore considered to be well converged.

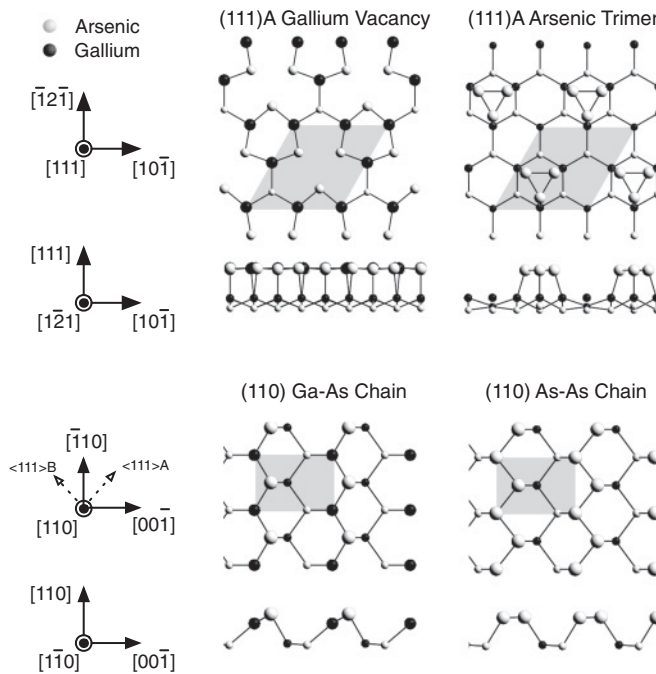


FIG. 2. Surface reconstructions/relaxations of the GaAs (111)A and (110) surfaces. Top left: the (111)A Ga vacancy surface. Top right: the (111)A As trimer surface. Bottom left: the (110) Ga-As chain surface. Bottom right: the (110)As-As chain surface. Arsenic atoms are light gray spheres and gallium atoms are dark gray spheres. Top and side views are rendered with two or three layers of atoms. The atomic diameters are drawn larger for atoms closer to the surface. The unit cell is identified by a shaded parallelogram or rectangle.

TABLE I. Calculated parameters for the (111)A surface. Diffusion barrier E_D , minimum potential energy A_1 , secondary minimum potential energy A_2 , and transition points T and T' of In and Ga adatoms. All values are in electronvolts (eV).

Surface	Adatom	E_D	E'_D	A_1	A_2	T	T'
Ga vacancy	Ga	1.06	1.14	-2.87	-2.21	-1.81	-1.73
	In	0.92	1.0	-2.65	-2.06	-1.73	-1.65
As trimer	Ga	0.27	-	-7.10	-	-6.83	-
	In	0.26	-	-6.99	-6.88	-6.73	-

III. RESULTS

The potential-energy surfaces for In and Ga adatoms above each surface reconstruction are presented in this section. The binding energies at adsorption sites A_i , transition points T and T' , primary diffusion barriers $E_D = T - A_1$, and secondary diffusion barriers $E'_D = T' - A_1$ for In and Ga above each surface are collected in Table I for the GaAs (111)A surface and in Table II for the GaAs(110) surface. The main results are that under As-rich conditions the diffusion barriers decrease, and the binding energy for In in the A_1 adsorption site is more competitive with Ga.

Comparing In and Ga adatoms above the Ga vacancy surface, see Fig. 3(a), the PES are qualitatively similar with a deep minimum at the vacancy site A_1 and a secondary minimum at the site A_2 above third layer As atoms. The transition points T and T' are saddle points of the PES that are crossed when hopping between adsorption sites, but the deep potential minimum makes atoms adsorbed onto this surface essentially immobile.

If atoms are able to overcome the deep potential well, diffusion can occur by two possible pathways. Either the adatom hops directly between A_1 sites over the transition point T' or it crosses over the point T into the secondary site A_2 and then rapidly hops back into an adjacent A_1 site. At typical growth temperatures of ~ 1000 K, diffusion between A_1 sites by way of A_2 is fast enough to dominate the diffusion path. The diffusion barrier E_D reported in Tables I and II is the barrier to hop from A_1 to A_2 .

Ga atoms are less mobile than In on this surface with a diffusion barrier 140 meV higher than In regardless of the path

TABLE II. Calculated parameters for the (110) surface. Diffusion barrier E_D , minimum potential energy A_1 , secondary minimum potential energy A_2 , and transition points T and T' of In and Ga adatoms. All values are in electronvolts (eV).

Surface	Adatom	E_D	E'_D	A_1	A_2	T	T'
Ga-As chain	Ga	0.22	0.57	-2.35	-	-2.13	-1.78
	In	0.23	0.52	-2.23	-	-2.00	-1.71
As-As chain	Ga	0.15	0.31	-2.50	-2.45	-2.35	-2.19
	In	0.12	0.38	-2.49	-2.44	-2.37	-2.11

taken. The binding energy of a Ga adatom at A_1 is 220 meV larger than for In, suggesting that Ga adatoms will be adsorbed preferentially over In adatoms. This calculation agrees with the observation that In floats to the surface when forming the NP heterointerface.⁹

The PES for a Ga adatom above the Ga vacancy reconstruction was previously calculated by Taguchi *et al.*¹⁷; however, our results are significantly different. In that work, contrary to expectations, they found the potential-energy minimum was not in the lattice site vacated by the Ga atom, but at adjacent interstitial locations with diffusion energy barriers of ~ 0.4 eV. Our calculations, in contrast, show a deep potential minimum at the vacant lattice site with diffusion barriers ~ 1.0 eV. We are unable to explain the discrepancies between the two calculations, however, the authors of Ref. 17 acknowledge that the vacant Ga site should be more stable according to calculations based on the interatomic potential. In light of the conflicting results, we carefully checked our energy calculations and algorithms for generating the PES, which exploit the surface symmetry, and are unable to find errors in our methods.

The As trimer PES for In and Ga adatoms are presented in Fig. 3(b). The As trimer surface is the stable reconstruction appearing in As-rich environments and is characterized by the presence of an As trimer to satisfy electron counting. The PES for both In and Ga adatoms have potential energy minimum A_1 at the center of the As trimer, and a diffusion barrier height of 260–270 meV. The PES for an In adatom also has a secondary minimum, A_2 , above one of the second layer As atoms that can potentially slow the diffusion for In. The difference in binding energy between Ga and In is only 110 meV for the As trimer

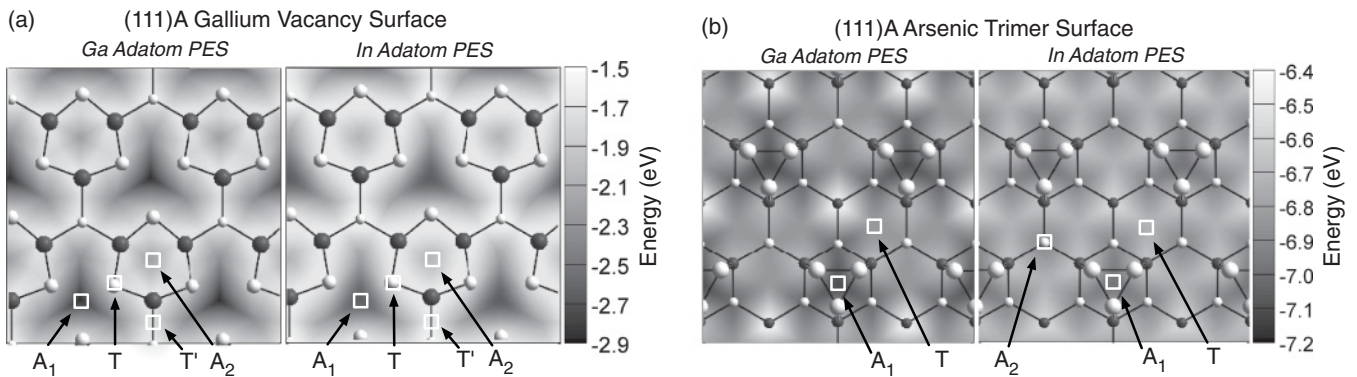


FIG. 3. Potential energy surface for Ga and In adatoms above the Ga vacancy surface and the As trimer surface (b). The top atomic layers of the reconstruction are drawn as an overlay to assist in visualizing the adsorption sites.

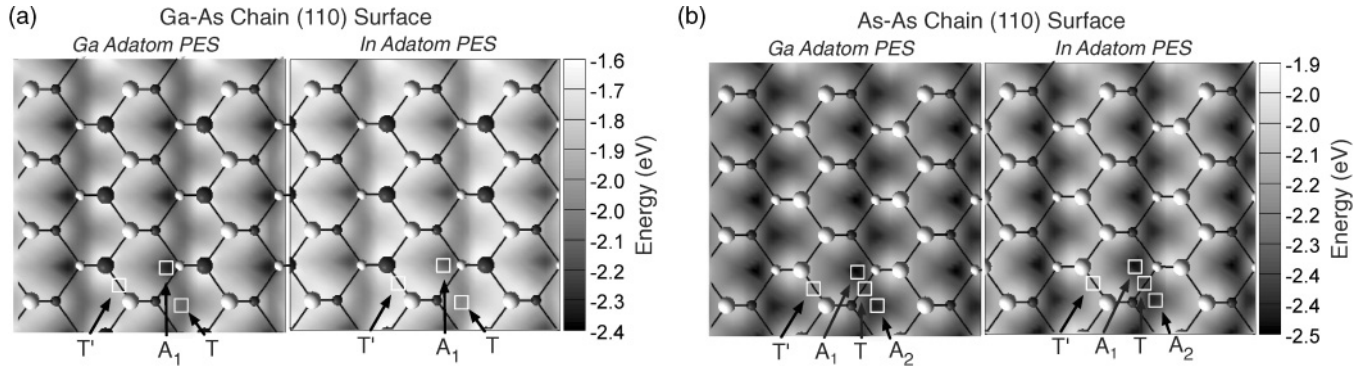


FIG. 4. Potential energy surface for Ga and In adatoms above the Ga-As chain surface (a) and the As-As chain surface (b). The top atomic layers of the reconstruction are drawn as an overlay to assist in visualizing the adsorption and transition sites. The primary and secondary adsorption sites are A_1 and A_2 , and the primary and secondary transition points are T and T' .

surface, compared to 220 meV for the Ga vacancy surface. Indium adatoms will have a higher probability of incorporation on this surface compared to the Ga vacancy surface because of the equivalent diffusion coefficients and more competitive binding energy.

The sidewalls of a pure zinc-blende NP are either the relaxed Ga-As chain or the As-As chain, as rendered in Fig. 2. The Ga-As chain surface is named for the chain of Ga and As atoms that run along the surface. When relaxed, the top layer Ga atom moves down so that the three bonds all lie in the same plane, and the As atom bonds approach ninety degrees. The surface resembles a trench-ridge structure.

The Ga-As chain PES, shown in Fig. 4(a), has an adsorption site in the trench adjacent to the As atom. The primary transition point also lies in the trench, but it is adjacent to the Ga atom. The diffusion barrier is comparable for In and Ga at 220 to 230 meV, suggesting that In and Ga have similar diffusion lengths on (110). In reality, the diffusion coefficient will vary with the vibrational free-energy of the atom, and change the diffusion barrier by as much as a few hundred meV.²² Even with this effect, diffusion is much faster on this surface than on the (111)A Ga vacancy surface, and it is highly anisotropic with atoms shuttled along the trenches.

In As-rich environments, the top-layer Ga adatom is replaced by an As atom creating an As-As chain. Like the Ga-As chain, the As-As chain PES has an adsorption site in the trench adjacent to the As atom, see Fig. 4(b), but a second adsorption site, A_2 , appears in the trench adjacent to the Ga atom. The diffusion barrier for travel along the trench is reduced to 150 and 120 meV for Ga and In adatoms, respectively. Twice as many barriers must be crossed to travel the same distance, but the lower diffusion barriers will result in significantly faster diffusion for both species.

Because the chains of the {110} surfaces are oriented at a 45° angle to the [111] direction, adatoms are shuttled up the trenches at an angle to the NP growth direction. At some point, adatoms must hop over the ridge into an adjacent trench to continue their diffusion toward the tip. The secondary diffusion barrier E'_D is the barrier to cross the ridge from the primary adsorption site A_1 over the secondary transition point T' . The As-As chain has a lower E'_D than the Ga-As chain by 260 and 140 meV for Ga and In respectively. The As-As chain has lower diffusion barriers

than the Ga-As chain both along the trench and over the ridge.

IV. DISCUSSION

Calculations were performed to provide a physical explanation to why As-rich conditions are required for the formation of GaAs/InGaAs axial heterostructures in (111)-oriented catalyst-free NPs. We believe that the high As chemical potential results in surface reconstructions on the NP that promote In incorporation on the (111) NP tip and simultaneously increase diffusion, and thus mass transfer of In adatoms along the {110} NP sidewalls.

The calculations reported in this work support the hypothesis that the (111) As-trimer surface, stable at high As chemical potential, is desirable for higher rates of In incorporation for two reasons. First, the difference in binding energy between Ga and In adatoms in the A_1 adsorption site is reduced from 220 meV on the Ga vacancy surface to 110 meV on the As trimer surface. This reduction means that In adatoms compete more effectively with Ga and have a higher probability of incorporating into the crystal. Second, the diffusion barriers E_D are comparable for both Ga and In adatoms on the As trimer surface, yet the diffusion coefficient of In is roughly two orders of magnitude larger on the Ga vacancy surface at typical growth temperatures of ~ 1000 K. On the Ga vacancy surface, In adatoms will diffuse more quickly than Ga and desorb more readily from the small (111) surface at the tip of the pillar. The resulting chemical environment of adsorbates at the pillar tip will be richer in Ga than in the surrounding vapor. In contrast, the comparable diffusion barriers of both Ga and In on the As trimer surface will result in a concentration of adsorbates representative of the concentration in the surrounding vapor. The two reasons cited explain why In adatoms incorporate more efficiently on the (111) surface at high As chemical potential.

At high As chemical potential the diffusion length of Ga and In adatoms on the (110) sidewalls increases. The As-As chain surface, with lower diffusion barriers both in the trenches and over the ridges is more efficient at shuttling adatoms to the NP tip. Upon arrival at the tip, In is then more likely to incorporate in the presence of an As-trimer surface.

V. SUMMARY

In summary, the PES for tracer In and Ga adatoms above stable surface reconstructions of GaAs (111)A and (110) are calculated. The binding energy of In is more competitive with Ga under As-rich conditions (high As chemical potential) on the (111)A As-trimer surface, and so it has more opportunity for incorporation into the lattice. Also at high As chemical potential, the NP (110) sidewall has lower diffusion barriers, and so the mass-transfer rate of atoms to the tip increases. The combined effects of higher mobility and more competitive binding energy indicates that formation of the (111)A As-

trimer surface and the (110) As-As chain under As-rich conditions can promote formation of axial GaAs/InGaAs heterointerfaces during nanopillar growth.

ACKNOWLEDGMENTS

The authors gratefully acknowledge the financial support of NSF (Grant Nos. DMR-1007051 and DMS-0439872), AFOSR (Grant Nos. FA9550-08-1-0198), DOD (Grant No. NSSEFF N00244-09-1-0091), and the NSF Clean-Green IGERT Fellowship funding for Mr. Shapiro (Grant No. DGE-0903720).

-
- ¹A. Fuhrer, L. E. Froberg, J. N. Pedersen, M. W. Larsson, A. Wacker, M.-E. Pistol, and L. Samuelson, *Nano Lett.* **7**, 243 (2007).
²J. Xiang, W. Lu, Y. Hu, Y. Wu, H. Yan, and C. M. Lieber, *Nature (London)* **441**, 489 (2006).
³W. Lu, J. Xiang, B. P. Timko, Y. Wu, and C. M. Lieber, *Proc. Natl. Acad. Sci. USA* **102**, 10046 (2005).
⁴M. Akabori, J. Takeda, J. Motohisa, and T. Fukui, *Nanotechnology* **14**, 1071 (2003).
⁵A. C. Scofield, J. N. Shapiro, A. Lin, A. D. Williams, P.-S. Wong, B. L. Liang, and D. L. Huffaker, *Nano Lett.* **11**, 2242 (2011).
⁶P. Senanayake, A. Lin, G. Mariani, J. Shapiro, C. Tu, A. C. Scofield, P.-S. Wong, B. Liang, and D. L. Huffaker, *Appl. Phys. Lett.* **97**, 203108 (2010).
⁷K. Ikejiri, T. Sato, H. Yoshida, K. Hiruma, J. Motohisa, S. Hara, and T. Fukui, *Nanotechnology* **19**, 265604 (2008).
⁸R. Agarwal, *Small* **4**, 1872 (2008).
⁹J. N. Shapiro, A. Lin, P. S. Wong, A. C. Scofield, C. Tu, P. N. Senanayake, G. Mariani, B. L. Liang, and D. L. Huffaker, *Appl. Phys. Lett.* **97**, 243102 (2010).
¹⁰H. Paetzelt, V. Gottschalch, J. Bauer, G. Benndorf, and G. Wagner, *J. Cryst. Growth* **310**, 5093 (2008).
¹¹A. Kley, P. Ruggerone, and M. Scheffler, *Phys. Rev. Lett.* **79**, 5278 (1997).
¹²K. Fujiwara, A. Ish, and T. Aisaka, *Thin Solid Films* **464-465**, 35 (2004).
¹³E. Penev, S. Stojković, P. Kratzer, and M. Scheffler, *Phys. Rev. B* **69**, 115335 (2004).
¹⁴M. Rosini, P. Kratzer, and R. Magri, *Phys. Status Solidi C* **7**, 181 (2010).
¹⁵M. Rosini, R. Magri, and P. Kratzer, *Phys. Rev. B* **77**, 165323 (2008).
¹⁶A. Taguchi, K. Shiraishi, and T. Ito, *Phys. Rev. B* **61**, 12670 (2000).
¹⁷A. Taguchi, K. Shiraishi, and T. Ito, *Phys. Rev. B* **60**, 11509 (1999).
¹⁸N. Moll, A. Kley, E. Pehlke, and M. Scheffler, *Phys. Rev. B* **54**, 8844 (1996).
¹⁹J. E. Northrup, *Phys. Rev. B* **44**, 1349 (1991).
²⁰V. Blum, R. Gehrke, F. Hanke, P. Havu, V. Havu, X. Ren, K. Reuter, and M. Scheffler, *Comput. Phys. Commun.* **180**, 2175 (2009).
²¹J. P. Perdew, K. Burke, and M. Ernzerhof, *Phys. Rev. Lett.* **77**, 3865 (1996).
²²U. Kürpick, A. Kara, and T. S. Rahman, *Phys. Rev. Lett.* **78**, 1086 (1997).